Pergamon

Adv. Space Res. Vol. 21, No. 12, pp. 1661–1664, 1998

0273-1177/98 $19.00 + 0.00

PII: S0273-1177(98)00010-6

AN INVESTIGATION OF THE SPATIAL VARIATIONS OF THE ENERGETIC TRAPPED ELECTRONS AT LOW ALTITUDES

S. F. Fung*, L. C. Tan*,**, D. Bilitza*,**, D. Boscher*,*** and J. F. Cooper*,**

**Space Physics Data Facility, NASA Goddard Space Flight Center, Greenbelt, MD 20771, U.S.A.*
***Also at the Hughes STX Corporation, Greenbelt, MD 20770, U.S.A.*
****On leave from CERT/ONERA, Toulouse, France*

ABSTRACT

We have analyzed the trapped electron data (0.19-3.2 MeV) taken by the Japanese OHZORA satellite operated at 350-850 km altitude in polar orbit during 1984-1987 near solar minimum. The electron observations reveal all the global attributes of the quiet-time electron radiation belts, such as the South Atlantic Anomaly, the electron "slot", and the outer radiation belt regions. The electron data are in general agreement with the NASA AE-8 electron model, but there are differences, particularly with respect to distinctive local-time variations in the slot region. In this paper, we present results from analyses of variations of the electron pitch angle distributions with local time, L-shell and altitude.

INTRODUCTION

The study of the trapped radiation is important because the radiation belts are integral parts of the Earth's magnetosphere; their structure and dynamics are intimately connected to and affected by many geophysical processes. For example, the energetic particles injected by geomagnetic storms and substorms into the equatorial magnetic traps in the inner magnetosphere can be permanently trapped if there are no external perturbations. On the other hand, the energetic trapped particles, having anisotropic velocity distributions, can interact with the background plasma to generate plasma waves and be pitch-angle scattered into the atmospheric loss cone. When the trapped particles reach their magnetic mirror points, they can also be scattered by the residual atmospheric particles through collisions. These scattering processes will cause the trapped particles to precipitate into the ionosphere and atmosphere, leading to a major source of ionization and energy deposition in these regions.

ANALYSIS OF OHZORA DATA

The Japanese OHZORA (EXOS-C) spacecraft was launched on February 14, 1984 into an orbit with an inclination of 75°, an apogee of 850 km, and a perigee of 350 km. The mission ended in March, 1987. The high energy particle (HEP) instrument on board consisted of two identical particle telescopes (Sensors 1 and 2). The OHZORA spacecraft was non-spinning (except for a five-day period; see below) with its orientation such that the field of view of Sensor 1 was fixed in the anti-sunward direction (the Z-axis) and that Sensor 2 was pointing perpendicular to Sensor 1.

Energetic electrons were detected by using the differential energy loss × total energy ($\Delta E \times E$) method. Electron identification was achieved by analyzing the signal from the ΔE detector, which has a 180 keV-threshold discrimination level for electrons. Electron energy was obtained by summing the signals from the ΔE and E detectors. Penetrating particles were discriminated by using an anticoincidence counter. The count rate saturated at about $5\times10^4\ s^{-1}$ (Kohno *et al.*, 1990). In most cases the count rate data of each telescope was output every 4 sec (the high time resolution mode). However, during some time intervals the signals were output every 16 sec (the low time resolution mode). The geometric factor and the acceptance half-cone angle of each telescope were 0.14 $cm^2 sr$ and 20°, respectively. Further details of the spacecraft and sensors were given by Nagata *et al.* (1985).

The trapped electrons are nominally identified by their strongly peaked pitch angle distributions in the direction normal to the local magnetic field. In a five-day interval (04/10/84 23:00:00 - 04/15/84 10:00:00) during a test phase of the OHZORA mission, the spacecraft was operating in a spinning mode which allowed the two orthogonal telescopes to sample many different pitch angles (Nagata *et al.*, 1985). With the HEP Sensor 1 fixed in the anti-sunward direction, its measured pitch angle is only slowly varying while Sensor 2 was freely rotating in the spin plane. If the anisotropic trapped electron distribution has a "$\sin^N\alpha$" profile, where α is the pitch angle of the electrons, one can determine the anisotropy index N from the ratio of the measurements of the two HEP sensors at two different pitch angles. Figure 1 shows the ratio of the count rates from the two HEP sensors as a function of the pitch angles observed by Sensor 2 (with α_1=79°). It is clear that the trapped electron pitch angle distribution can be modeled by a "$\sin^N\alpha$" profile with N=5.5. We note also that the locally observed loss cone threshold, given by α_{th}, is typically smaller than the critical loss cone angle α_c given by the local magnetic mirror ratio based on the conservation of the first invariants (Roederer, 1970). Using 111 similar events observed during the spinning period, we have obtained an average loss cone angle $<\alpha_{th}> = 27 \pm 6$ (°) and an average anisotropy index $<N> = 4.7 \pm 1.4$, consistent with the average value of $N = 5$ found by Kohno *et al.* (1990).

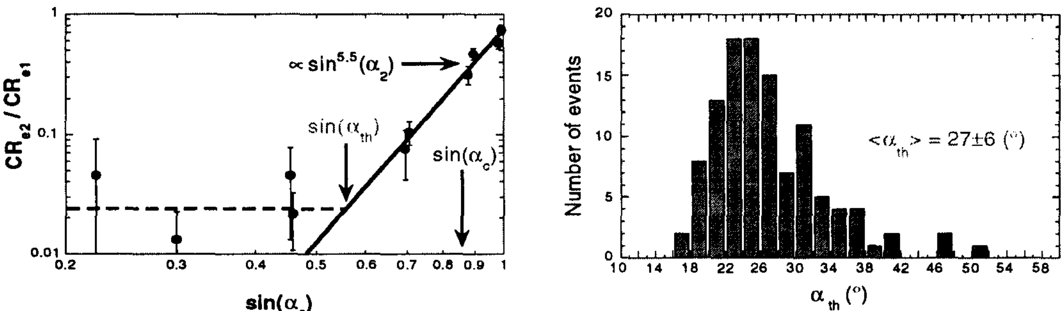

Fig. 1. Left panel is an example of the anisotropic pitch angle distributions observed by OHZORA during its spinning operation period (April 13, 1984; 19:24:43-19:25:31 UT); the right panel shows the histogram of the threshold pitch angle within precipitating particles are observed.

Based on the observed average loss cone angle, we have selected for this study only the events for which both telescopes were sampling outside the threshold angle $\alpha_{th} = 27 + 6 = 33°$, i.e., only within the quasi-trapped or trapped electron distributions. In addition, due to the axial symmetry of the assumed pitch angle distribution, significant errors in the calculation of N may result if the difference between $\sin(\alpha_1)$ and $\sin(\alpha_2)$ was too small. Thus we have also resticted our data selection to using only the events with $\Delta\alpha > 15$ °, where $\Delta\alpha$ is the smaller of the two quantities $|\alpha_1 - \alpha_2|$ and $|\pi - \alpha_1 - \alpha_2|$.

SPATIAL VARIATIONS OF TRAPPED ELECTRONS AT LOW ALTITUDES

For the purpose of this study, only the OHZORA trapped electron observations (1984-87) obtained during nominally quiet conditions with $|D_{st}| <$ 30nT were used. Upon determining the anisotropy indices N assoicated with the observed trapped electron events, the omnidirectional fluxes can be calculated by integrating over the corresponding $\sin^N\alpha$ profile. The global distributions of the trapped electron omni-directional fluxes between 0.19-3.2 MeV at 400 km and 800 km are shown in Figure 2. The canonical inner and outer electron belt structures are clearly seen in the figure. The inner electron belt is limited to the longitude range of the South Atlantic Anomaly (SAA) region with enhanced peak fluxes at higher altitudes. In a recent study, Fung *et al* (1996) showed that the L-profiles of the omnidirectional trapped electron fluxes computed from the AE-8 MIN model are generally consistent with those observed by OHZORA above the magnetic (or atmospheric) cutoff. In the following, we discuss some spatial variations of the trapped electrons seen in the low-altitude OHZORA observations.

The long-term OHZORA observations allow us to investigate the variations of the pitch angle distributions. Figures 3a and 3b display the local-time variations of the omnidirectional fluxes (left panel) and the associated anisotropy indices N (right panel) of the trapped electrons for different L ranges. In the high L region (e.g., $L > 6.5$), the omnidirectional fluxes tended to a maximum near local noon, apparently caused by the longitudinally asymmetric drift action of the trapped electrons near the outer boundary of the radiation belt (Roederer, 1970). In the middle L region ($4.0 < L < 6.5$), the electron fluxes became more uniform over local time, indicating that the electron drift paths were closed and symmetric. The pitch angle distributions of these particles however exhibit a systematic change with local time with the local noon particles becoming more isotropic (*i.e.*, smaller N values). In the low L-shell range ($L < 4.0$), the local-time variations of the electron distributions have clearly changed to the local noon sector having a minimum flux and minimum N. These tendencies are most visible in the slot region near $2.0 < L < 3.0$.

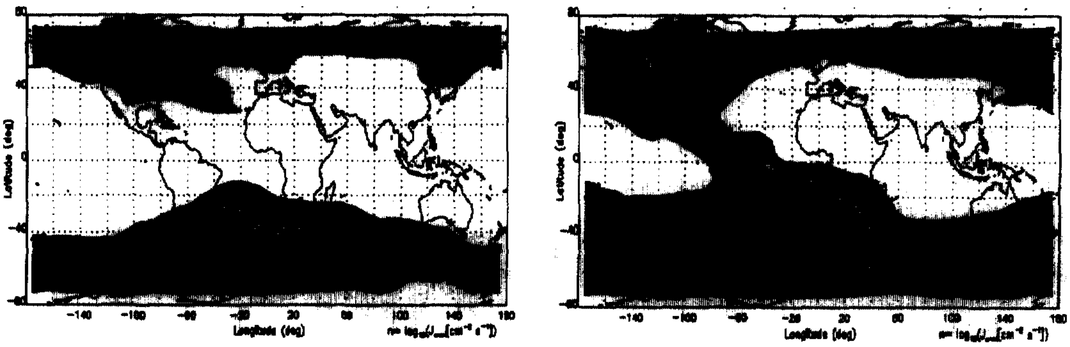

Fig. 2. Global trapped electron distributions (0.19 -3.2 MeV) observed by OHZORA at 400 km (left panel) and 800 km (right panel), respectively, in 1984-87.

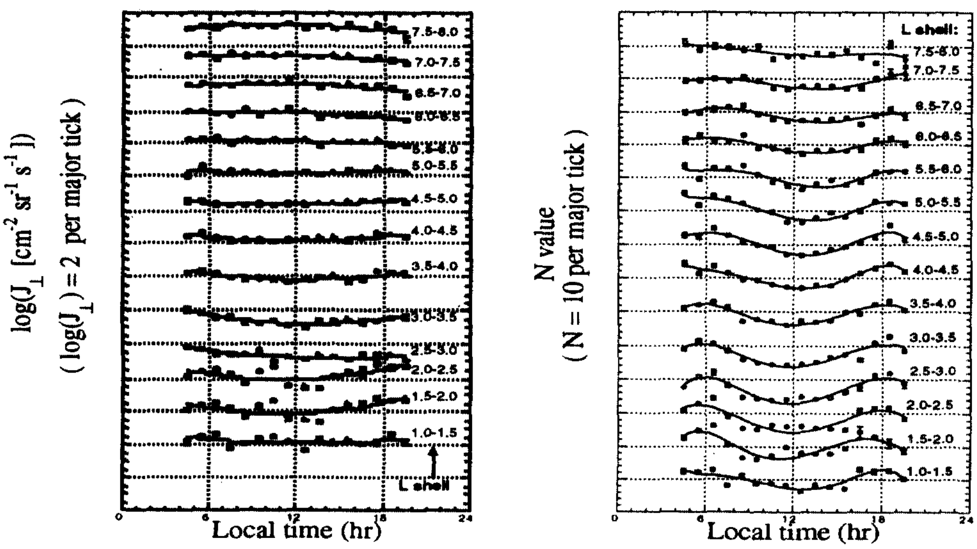

Figs. 3a and 3b. Local-time variations of omnidirectional fluxes (left panel) and anisotropy indices N (right panel) of the trapped electrons (0.19 < E < 3.2 MeV) observed by OHZORA during nominally quiet times (|Dst| < 30 nT) in 1984-87.

It is also informative to examine the local-time variation in the structure of the slot region. Since the slot is believed to be created by wave-particle interaction processes (Lyons *et al.*, 1972), the local time structure of the slot will indicate the extent of the wave-particle interaction region. Figure 4 shows the L profiles of the trapped electron fluxes in different local time zones observed at low altitudes. The top three panels show the comparisons of the L profiles taken from local time zones symmetric about local noon while the bottom panel displays the profile near local noon. The panels in Figure 4 reveal that the overall slot structure is fairly symmetric about local noon. In addition, the slot region tends to widen and become more evacuated toward noon while the slope of the inner edge of the slot becomes more gentle or eroded. Such variations in the slot structure must be related to the plasmaspheric hiss wave distribution at higher altitudes.

Since the local-time variations shown in Figs. 3 and 4 are revealed in the long-term observations, they are likely to be steady features associated with quiet times. These features, however, are not readily explainable in terms of drift shells, particularly in the low L region. The tendency toward more isotropic distributions (smaller N) and an extensive slot near local-noon may indicate stronger plasmaspheric hiss activity in this local-time sector.

SUMMARY

The spatial variations of trapped electrons at low altitudes (350-850 km) have been investigated by using the OHZORA observations taken near solar minimum (1984-87). Understanding the causes of these variations will be important for identifying the physics which controls the occurrence and loss of the trapped electrons and for developing a semi-empirical, magnetospheric state-based trapped radiation model (Boscher *et al.*, 1996; Fung, 1996).

Figure 2 shows that the omnidirectional flux of trapped electrons increases with altitude, particularly in the SAA region. Such tendency may result from a combination of higher atmospheric scattering and larger local loss cone angles at lower altitudes. What is not clear is the cause of the local-time variations in the pitch angle distributions in the low *L* range (Fig. 3). Since the geomagnetic field is fairly symmetric in this region, drift loss cone effect (Roederer, 1970) should be minimal. The different anisotropies and slot structure (Fig. 4) occurring at different local times suggest that particle dynamics are affected by local processes operating over long time scales and that the electrons are not stably trapped at these *L* values.

Recently, it has been shown that the quiet-time L-profiles of omnidirectional electron fluxes computed from the AE-8MIN model are generally consistent with the long-term OHZORA observations at L > 3 (Fung *et al.*, 1996; Boscher *et al.*, 1996). Discrepancies, such as a shift of the slot region by as much as $\Delta L \approx 0.5$, between the observations and the model have been noted at lower L. Some of these discrepancies may be resolved by properly modeling the spatial variations of the trapped electrons, such as those discussed here.

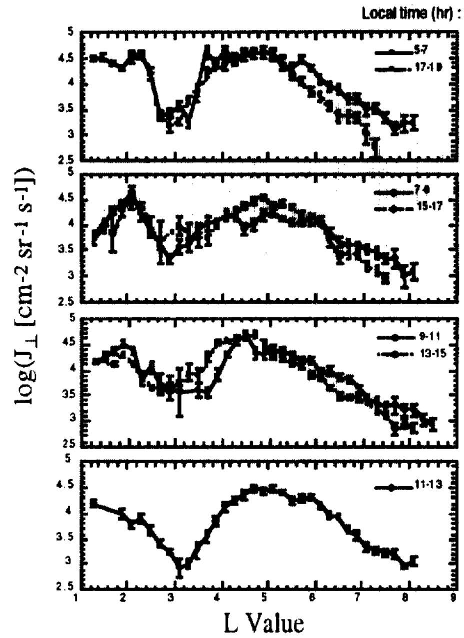

Fig. 4. L-profiles of trapped electron fluxes observed in different local time zones.

ACKNOWLEDGEMENTS

We thank Drs. T. Kohno (IPCR, Saitama, Japan) and K. Nagata (Tamagawa University, Tokyo, Japan) for providing the OHZORA data to the National Space Science Data Center (NSSDC).

REFERENCES

Boscher, D. M., S. F. Fung, and L. C. Tan, Spatial distributions of the inner radiation belt electrons: a comparison between observations and radial diffusion theory predictions, *Adv. Space Res.*, to be published (1996).

Fung, S. F., Recent development in the NASA trapped radiation models, *Radiation Belts: Models and Standards*, Geophysical Monogr., **97**, AGU, Washington, D. C., 79-91 (1996).

Fung, S. F., D. M. Boscher, L. C. Tan, J. F. Cooper, and D. S. Evans, Modeling the low-altitude trapped radiation environment, *ESA Symposium Proc. 'Environment Modelling For Space-Based Applications'*, SP-392, ESTEC, Noordwijk, the Netherlands, 65-74 (1996).

Lyons, L. R., R. M. Thorne, and C. F. Kennel, Pitch-angle diffusion of radiation belt electrons within the plasmasphere, *J. Geophys. Res.*, **77**, 3455 (1972).

Nagata, K., T. Kohno, H. Murakami, A. Nakamoto, N. Hasebe, T. Takenaka, J. Kikuchi, and T. Doke, OHZORA high energy particle observations, *J. Geomag. Geoelectr.*, **37**, 329 (1985).

Kohno, T., K. Munakata, K. Nakada, H. Murakami, A. Nakamoto, N. Hasebe, J. Kikuchi, and T. Doke, Intensity maps of MeV electrons and protons below the radiation belt, *Planet. Space Sci.*, **38**, 483 (1990).

Roederer, J. G, *Dynamics of Geomagnetically Trapped Radiation*, Springer-Verlag, New York (1970).